

Radar echoes from the icy Galilean satellites—Europa, Ganymede, and Callisto—are unique in character, and they may be explained by a phenomenon that has been called the radar glory effect.<sup>1,2,3,4</sup> We have analyzed the radar glory backscattering from buried craters as a possible model for this effect. These craters have a smaller refractive index below the crater than above as shown in Fig. 1(A). The possibility exists that the rays shown will be totally internally reflected at the crater walls, and we assume this to be true in the following. The rays which contribute to the backscattering will come from a circular annulus, when viewed before the refraction occurs at the ice-vacuum surface, in a plane orthogonal to the rays reflected from the crater (see Fig. 1(B)). For craters near the limb of the satellite some of the rays may be blocked by the crater rim, and this circular annulus will break up into two circular arcs. We assume that these glory arcs are broken up into glints of dimension  $H$ , assumed larger than the wavelength, and that the fields from a pair of glints connected by the ray shown add coherently while the fields from the various glint pairs add incoherently. The coherent addition of the fields from glint pairs arises because for the ray shown in Fig. 1(A), there is another ray that travels the exact same path, but in the opposite direction.

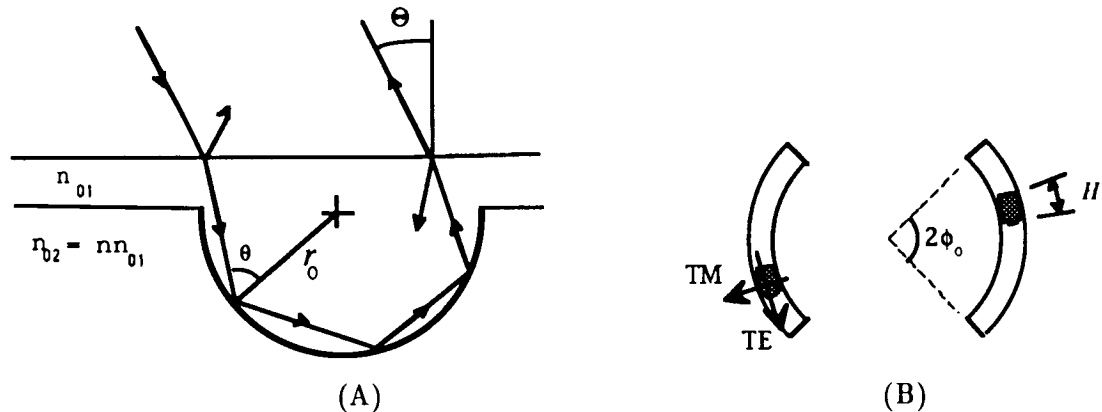


Figure 1. (A) Geometry of a buried crater and a three-bounce ( $N=3$ ) ray. The angle  $\Theta$  is between the surface normal of the satellite and the radar line of sight. For an ice-overburden,  $n_{01} = 1.8$ . In the model  $n_{02} < n_{01}$  (i.e.,  $n < 1$ ). (B) Glory arcs of angular extent  $2\phi_0$  and a pair of glints of dimension  $H$ . TE and TM electric field vectors are also shown.

Consider a crater located near the surface of the satellite at coordinates  $(R, \Theta, \Phi)$ , where  $R$  is the satellite radius,  $\Theta$  is longitude with  $\Theta = 0$  in the direction of Earth, and  $\Phi$  is latitude with  $\Phi = \pi/2$  in the plane defined by the spin axis of the satellite and the  $\Theta = 0$  direction. The radar cross-sections for fields received in the orthogonal and same linear (OL and SL respectively) polarizations and those for fields received in the orthogonal and same circular (OC and SC respectively) polarizations are

$$\sigma_{SL}(\Theta, \Phi) = CA_L(3 - X_L) \quad , \quad \sigma_{OL}(\Theta, \Phi) = CA_L(1 + X_L) \quad (1)$$

$$\sigma_{SC}(\Theta) = 2CA_C(1 + X_C) \quad , \quad \sigma_{OC}(\Theta) = 2CA_C(1 - X_C). \quad (2)$$

The constant  $C$  is proportional to the number of glint pairs in the glory arcs, and is given by  $C = \pi r_0^2 FH/\lambda$  where  $F$  is the fraction of the glory arcs filled by glints,  $H$  is defined in Fig. 1(B), and  $\lambda$  is the radar wavelength. The  $A$ 's and  $X$ 's are given by

$$A_L = \frac{1}{2} \hat{\sigma}_0 \{ [(T_1^2 + T_2^2) + (T_1^2 - T_2^2) \cos 2(\Phi - \Phi_P)] [\phi_0 - (1+x)\delta] + 2T_1 T_2 (1+x)\delta \} \quad (3)$$

$$A_L X_L = \hat{\sigma}_0 \{ 2T_1 T_2 x \phi_0 + [(T_1^2 - T_2^2) \cos 2(\Phi - \Phi_P) - (T_1^2 + T_2^2) \cos 4(\Phi - \Phi_P)] [\phi_0 - (1+x)\delta] + 2T_1 T_2 [3(1+x)\delta - x\phi_0] \cos 4(\Phi - \Phi_P) \} \quad (4)$$

$$A_C = \hat{\sigma}_0 \{ (T_1^2 + T_2^2) \phi_0 - (T_1 - T_2)^2 (1+x)\delta \} \quad (5)$$

$$A_C X_C = 2\hat{\sigma}_0 T_1 T_2 x \phi_0 \quad (6)$$

where

$$\hat{\sigma}_0 = \frac{\sin 2\theta}{N} \frac{\cos^2 \Theta}{n_{01}^2 \cos^2 \Theta'}, \quad (7)$$

$n_{01} \sin \Theta' = \sin \Theta$ ,  $\Phi_P$  is the direction of polarization for the linear polarization case,  $T_1 = 4n_{01} \cos \Theta \cos \Theta' / (\cos \Theta + n_{01} \cos \Theta')^2$  is the product of the TE Fresnel transmission coefficient for the ray entering the ice and the TE Fresnel transmission coefficient the ray exiting the ice,  $T_2 = 4n_{01} \cos \Theta \cos \Theta' / (n_{01} \cos \Theta + \cos \Theta')^2$  is the same product for the TM fields,  $x = \cos[2N \tan^{-1}(\cos \theta (\sin^2 \theta - n^2)^{1/2} / \sin^2 \theta)]$  is the mode decoupling factor defined in reference 1,  $\delta = \phi_0/4 - \sin(4\phi_0)/16$ , and  $\phi_0 = \pi/2$  if no shadowing occurs or  $\sin \phi_0 = \cot \theta \cot \Theta'$  when this last definition has a real solution.

The power spectra are sums of the contributions from several craters along lines of constant Doppler shift which are lines, when projected onto the plane of the sky, orthogonal to the line of sight and parallel to the spin axis. That is, the cross-sections at a specified frequency are integrals of the cross-sections in equations (1) and (2) on semi-circles on the satellite surface where  $\cos \Theta \cos \Phi = \text{constant}$ . In Fig. 2 we compare the computed cross-section for circular polarization with echoes obtained from Eurpoa; this spectrum is typical of the spectra obtained.

The total cross-section of each satellite is an integration of the cross-sections in equations (1) and (2) over the entire illuminated surface. These total cross-sections can be written in a form similar to those in equations (1) and (2) except that the  $A$ 's and  $X$ 's are the same for linear and circular polarizations and are complicated integrals that must be computed numerically. In Table 1 we compare a summary of the main features of the data with the model predictions. The scaling constant  $C$  for these total cross-sections is given by  $C = (M\pi r_0^2/4\pi R^2)(FH/\lambda)$  where  $M$  is the total number of craters on the surface.

**ACKNOWLEDGEMENTS:** This research was supported by NASA grants NGL-05-020-014 and NGT-70056 and NSF grant AST 87-21880.

**REFERENCES:** <sup>1</sup>Eshleman (1986), *Science* **234**, 587. <sup>2</sup>Eshleman (1986), *Nature* **319**, 755. <sup>3</sup>Eshleman (1987), *Advances in Space Research* **7.5**, 133. <sup>4</sup>Gurrola and Eshleman (1990), *Advances in Space Research* **10.1**, 195. <sup>5</sup>Ostro (1982), chapter 8 in *Satellites of Jupiter*, edited by D. Morrison, University of Arizona Press, Tucson.

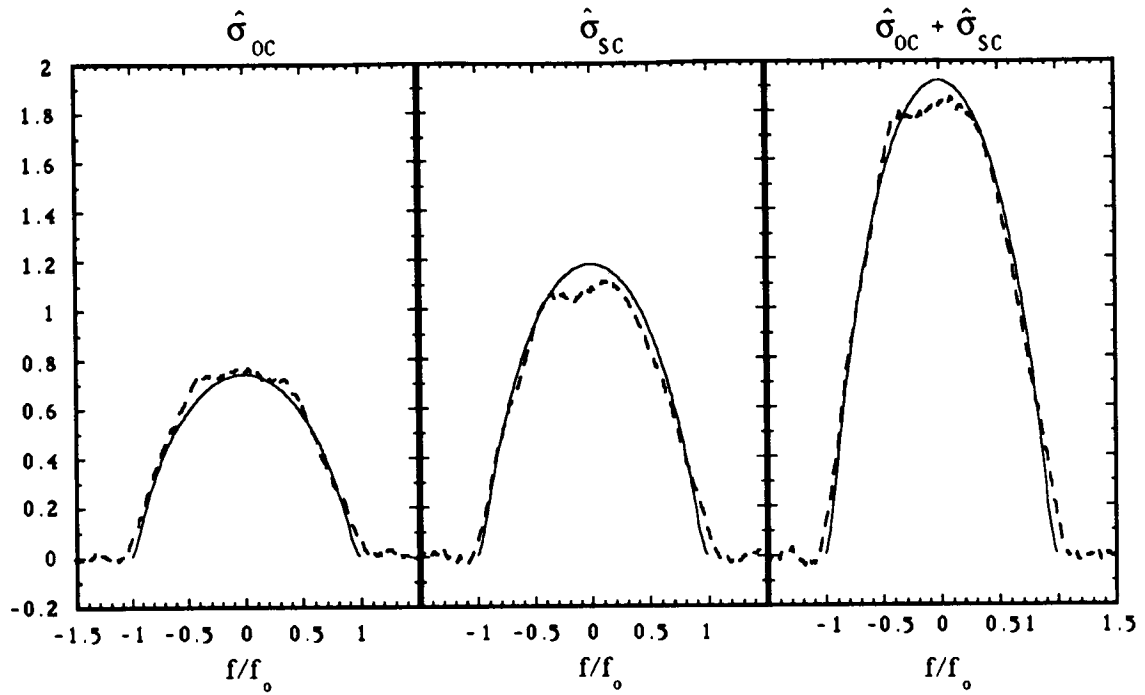


Figure 2. OC, SC, and OC+SC cross-sections obtained from Europa (dashed curves) on January 10, 1990 at the Arecibo Observatory at 12.6 cm- $\lambda$  and from the model (solid curves) using  $N = 3$ ,  $n=0.7967$ . The data and the model have been scaled to give a total cross-section of 2.6.

	Europa	Ganymede	Callisto	Buried craters $N = 3, n=0.7967, C = 1$
$\hat{\sigma}$	2.60	1.52	0.64	0.67
$\hat{\sigma}_{SC}/\hat{\sigma}_{OC}$	1.56	1.55	1.19	1.60
$\hat{\sigma}_{OL}/\hat{\sigma}_{SL}$	0.47	0.47	0.55	0.44
m	1.73	1.46	1.43	1.95

Table 1: The data for the Galilean satellites are for 12.6 cm- $\lambda$  and are from Ostro<sup>5</sup>.  $\hat{\sigma} = \hat{\sigma}_{SC} + \hat{\sigma}_{OC} = \hat{\sigma}_{SL} + \hat{\sigma}_{OL}$ . These cross-sections are normalized by the geometrical area  $\pi R^2$ , i.e.,  $\hat{\sigma} = \sigma/\pi R^2$ . Here m is the exponent for a least squares fit of the power spectra to a  $\cos^m \Theta$  law.